

WONYONG KWON<sup>1</sup>, YOUNGMIN KIM<sup>1</sup>, MINJU SON<sup>1</sup>, EUI SEON LEE<sup>1</sup>, SUNG-TAG OH<sup>1\*</sup>

## NON-ISOTHERMAL REDUCTION BEHAVIOR AND MICROSTRUCTURAL CHARACTERISTICS OF MoO<sub>3</sub> POWDER IN PURE HYDROGEN ATMOSPHERE

The reduction behavior and microstructure of both raw and ball-milled MoO<sub>3</sub> powders have been investigated. The raw powder consisted of coarse plate-shaped particles, whereas the powder ball-milled for 5 h showed agglomerates composed of fine equiaxed particles. XRD analysis of the hydrogen-reduced powders indicated that only the diffraction lines for Mo are observed. In contrast, the milled powder exhibited the main peak of Mo and carbides peak as minor phases. The reduction kinetics of MoO<sub>3</sub> powders were evaluated by analyzing the extent of peak shift at various heating rates using thermogravimetric analysis. The activation energies for the raw powder were determined to range from 97.5 to 104.4 kJ/mol, which are approximately consistent with the values reported for the isothermal reduction of MoO<sub>3</sub> in a hydrogen atmosphere. For the ball-milled powders, the activation energy was measured to be 148.8-167.1 kJ/mol, which was interpreted to be related to the carbides formed by the reaction of Fe and C impurities with Mo.

*Keywords:* MoO<sub>3</sub> powder; ball milling; hydrogen reduction; activation energy; microstructure

### 1. Introduction

Molybdenum (Mo) is a valuable refractory metal for high-temperature applications due to its unique physical, chemical, and mechanical properties [1,2]. Because Mo has a high melting point of 2610°C, powder metallurgy has been widely established as a process for producing bulk components. However, sintering of commercial Mo powder with a particle size of several micrometers requires a high temperature near 2000°C and a long time [3,4]. This process results in significant grain coarsening, which subsequently leads to the deterioration of mechanical properties. To enhance sinterability at low sintering temperatures and suppress grain growth, several novel methods, such as activated sintering, nano-sintering, and pressure sintering, have been proposed [5-7].

Since the driving force for sintering is mainly determined by the reduction in surface energy and curvature of the powder [6], minimizing particle size can significantly improve the sinterability. Thus, nano-sintering using ultrafine powders is regarded as a promising method to enhance densification at relatively low temperatures. In this regard, the process of ball milling MoO<sub>3</sub> powder followed by hydrogen reduction has been developed to produce ultrafine Mo powder [8]. Considering the dependence of processing conditions on the microstructure of the prepared

powder, it is essential to understand the milling process and hydrogen reduction behavior of the metal oxide to synthesize ultrafine metal powder with the required properties. This study investigates the reduction behavior of ball-milled MoO<sub>3</sub> powder by thermogravimetric analysis at various heating rates in a pure hydrogen atmosphere. Furthermore, the influence of powder processing conditions on the microstructure of the synthesized powder is examined.

### 2. Materials and methods

The starting material used was molybdenum trioxide (MoO<sub>3</sub>, 99.9%, 1-5 μm, Kojundo Chemical Lab. Co.). The raw powder and balls of 3 mm in diameter were placed into a jar with high purity methanol. The milling was conducted using a planetary ball mill at 400 rpm for 5 h with a ball to powder weight ratio of 15:1, and the balls and jar were made of hardened steel. Stearic acid, equivalent to 1 wt.% of the total powder, was incorporated as a process control agent to inhibit excessive cold welding of powders.

The reduction behavior of ball-milled MoO<sub>3</sub> powders was evaluated using a thermogravimetric analysis (TGA, Thermo

<sup>1</sup> SEOUL NATIONAL UNIVERSITY OF SCIENCE AND TECHNOLOGY, DEPARTMENT OF MATERIALS SCIENCE AND ENGINEERING, SEOUL 01811, REPUBLIC OF KOREA

\* Corresponding author: [stoh@seoultech.ac.kr](mailto:stoh@seoultech.ac.kr)



plus EVO2, Rigaku) from room temperature to 900°C at heating rates of 2, 5, 10 and 20°C/min in a hydrogen atmosphere with a purity of 99.999%. For comparative purposes, raw MoO<sub>3</sub> powder was analyzed under identical conditions. Phase identification of the powders was performed using X-ray diffraction (XRD, Dmax 2500, Rigaku) analysis. The morphology of powders was examined via field-emission scanning electron microscopy (FE-SEM, JSM-6700F, JEOL). The size distributions of the powders were determined by dynamic light scattering using nano SAQLA (Otsuka Denshi).

### 3. Results and discussion

Typical SEM image and particle size distribution of the raw and ball-milled MoO<sub>3</sub> powders are shown in Fig. 1(a) and (b), respectively. The raw MoO<sub>3</sub> powder is characterized by coarse plate-shaped particles, whereas the powder subjected to ball milling for 5 h exhibits agglomerates composed of fine equiaxed particles. As shown in Fig. 1, both powders have bimodal size distributions, with peak sizes of 0.09 and 0.34 μm for the milled powder, which are significantly smaller than those of 0.61 and 26.4 μm for the raw powder.

The hydrogen reduction behavior of MoO<sub>3</sub> powders was investigated by non-isothermal TGA at various heating rates from room temperature to 900°C. Fig. 2(a) and (b) show the TG curves for the relative weight and derivative weight loss during the heating process of raw and ball-milled powders, respectively. As can be seen from the relative weight curves in Fig. 2(a), the

onset temperature of weight loss for the raw powder is in the range of 490–620°C, which is higher than the range of 350–430°C observed in the milled powder. According to the literature [9], the reduction of MoO<sub>3</sub> to MoO<sub>2</sub> by hydrogen occurs within the temperature range of 350°C to 600°C, while the deoxidation of MoO<sub>2</sub> to Mo takes place from 600°C to 850°C. Therefore, the onset temperature depicted in Fig. 2(a) can be primarily ascribed to the reduction process of MoO<sub>3</sub> to MoO<sub>2</sub>. However, further analysis is necessary to elucidate the relatively low onset temperature observed in the milled powder.

Fig. 3(a) shows the XRD profile of the ball-milled powder after heating to 412°C at a rate of 5°C/min, which corresponds to the temperature of  $T_{m3}$  indicating the maximum weight loss rate in Fig. 2(b). Diffraction lines corresponding to MoO<sub>3</sub> were identified in the ball-milled powder. After heat treatment at 412°C in a hydrogen atmosphere, the MoO<sub>3</sub> peak was no longer detectable, and only the diffraction lines for the MoO<sub>2</sub> and MoOC phases were observed. The MoO<sub>2</sub> phase is attributed to an intermediate phase formed through stepwise reduction of MoO<sub>3</sub>. Meanwhile, the formation of MoOC is believed to be the result of a reaction with carbon impurities introduced during the milling process using stainless steel balls and jar. The XRD results of the powder heated to the temperature at which the reduction reaction was completed are shown in Fig. 3(b). In the raw powder, only the diffraction lines for Mo are observed, whereas the main peak in the milled powder corresponded to Mo, and the peaks of Mo<sub>2</sub>C and Fe<sub>3</sub>Mo<sub>3</sub>C were visible as minor phases. Based on the results of the XRD analysis, the initiation of hydrogen reduction in the milled powder at a relatively low temperature, as depicted

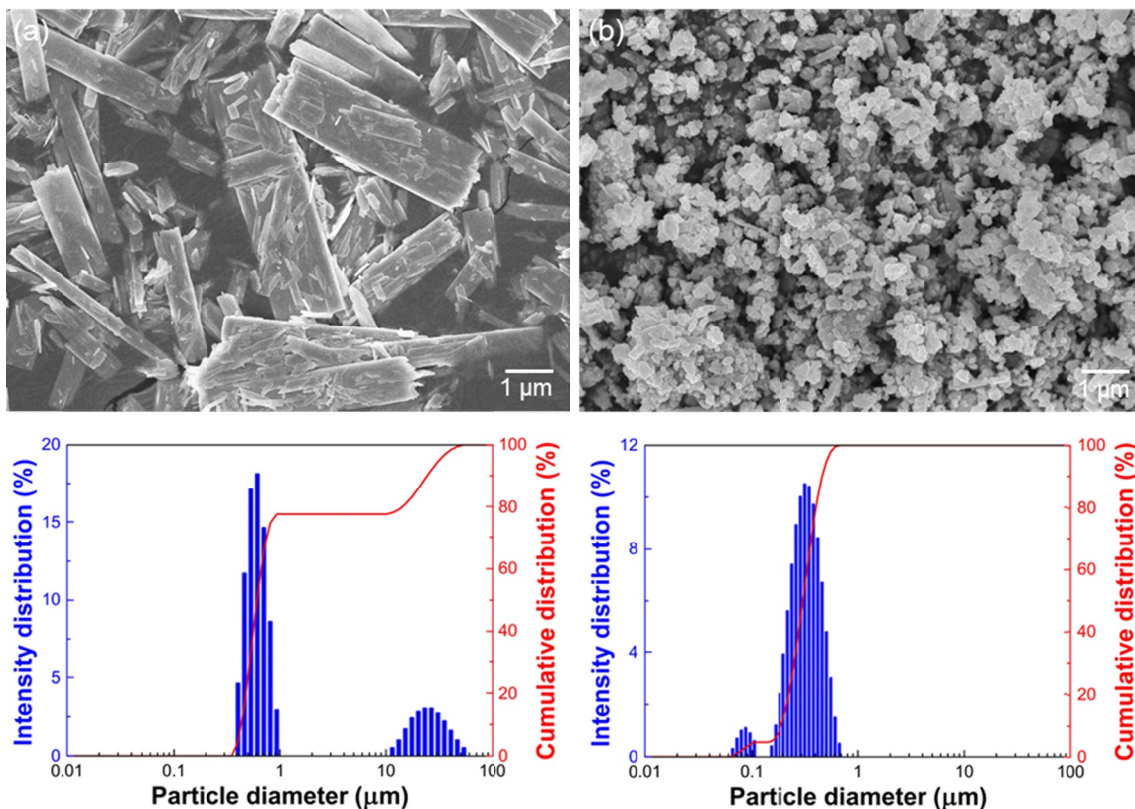


Fig. 1. SEM micrographs and particle size distribution curves of (a) raw and (b) ball-milled MoO<sub>3</sub> powder

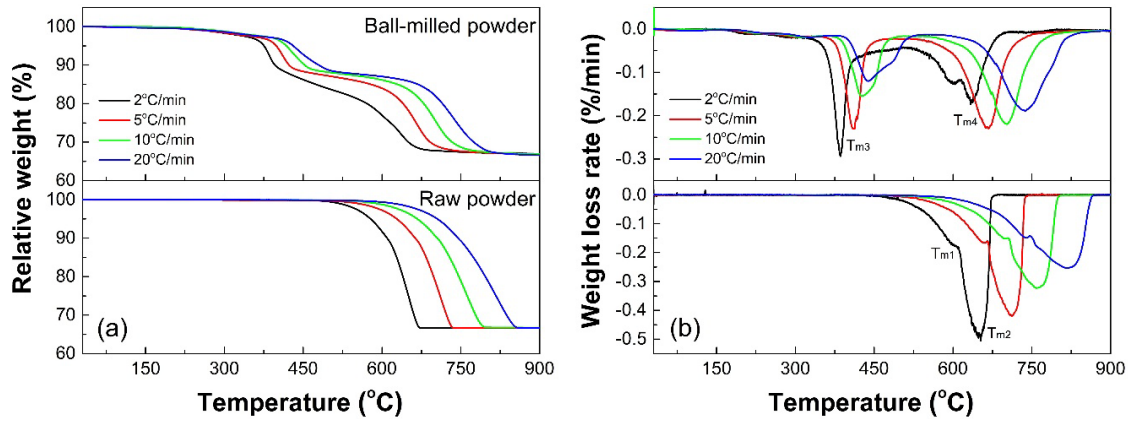


Fig. 2. (a) TG and (b) differential TG curves of raw and ball-milled  $\text{MoO}_3$  powders, scanned at various heating rates in hydrogen atmosphere

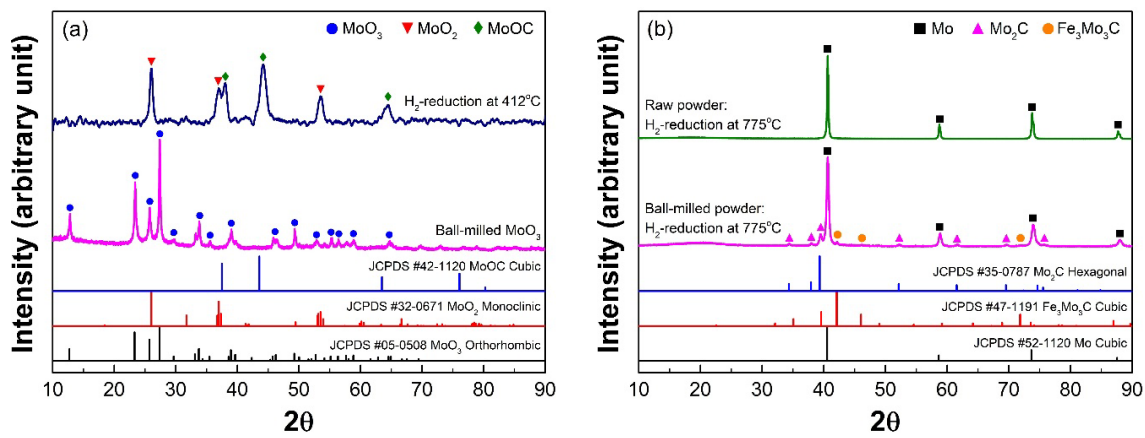


Fig. 3. XRD profiles of  $\text{MoO}_3$  powder at various processing stages: (a) ball milling and hydrogen reduction at  $412^\circ\text{C}$ , (b) hydrogen reduction of both raw and ball-milled powder at  $775^\circ\text{C}$  for 1 h

in Fig. 2, is interpreted as being mainly due to the refinement of particles by ball milling and the presence of impurity carbon.

The reduction kinetics of  $\text{MoO}_3$  powders were assessed by examining the extent of peak shift at various heating rates in TGA. As shown in Fig. 2(b), the peak temperature ( $T_m$ ), corresponding to the maximum rate of weight loss, shifts to higher temperatures as the heating rate increases. In non-isothermal mode, the Kissinger method determines the apparent activation energy assuming that the reaction rate reaches a maximum at the peak temperature [10]:

$$\ln\left(\frac{\beta}{T_m^2}\right) = -\frac{Q}{R} \cdot \frac{1}{T_m} + \text{constant}$$

where  $\beta$  represents the heating rate,  $T_m$  denotes the peak temperature and  $R$  is the gas constant. Therefore, the apparent activation energy ( $Q$ ) for the hydrogen reduction process can be determined from the slope of a plot of  $\ln(\beta/T_m^2)$  against  $1/T_m$ , as shown in Fig. 4.

For the raw powder, the activation energies corresponding to the peak temperatures  $T_{m1}$  and  $T_{m2}$  were measured to be 104.4 kJ/mol and 97.5 kJ/mol, respectively. The values obtained are approximately consistent with the reported activation energies for the isothermal reduction of  $\text{MoO}_3$  in a hydrogen at-

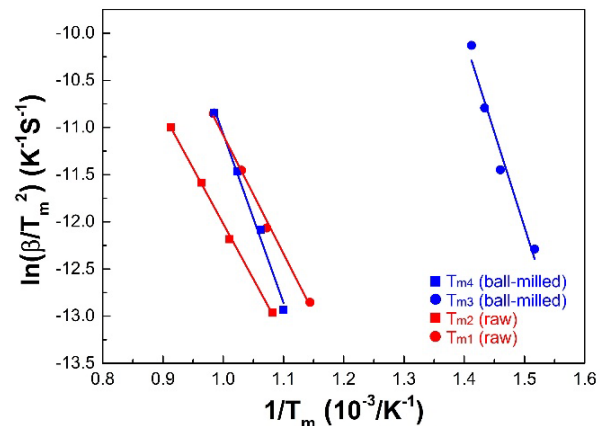


Fig. 4. Kissinger plots for the reduction of raw and ball-milled  $\text{MoO}_3$  powders

mosphere: 114–122 kJ/mol for the  $\text{MoO}_3 \rightarrow \text{MoO}_2$  process [11] and 92.5 kJ/mol for the  $\text{MoO}_2 \rightarrow \text{Mo}$  process [12]. Meanwhile, the activation energies for the peak temperatures  $T_{m3}$  and  $T_{m4}$  in the ball-milled powder were determined to be 167.1 kJ/mol and 148.8 kJ/mol, respectively. The higher activation energy of the ball-milled powder compared to the raw powder can be interpreted as due to the formation of carbides resulting from the reaction between Fe and C impurities with Mo.

#### 4. Conclusions

This study focused on the characterization and understanding of the hydrogen reduction behavior of MoO<sub>3</sub> powders. The raw MoO<sub>3</sub> powder is characterized by coarse plate-shaped particles, whereas the powder subjected to ball milling for 5 h exhibits agglomerates composed of fine equiaxed particles. The hydrogen reduction behavior of MoO<sub>3</sub> powders was investigated by non-isothermal TGA at various heating rates from room temperature to 900°C. The onset temperature of weight loss for the raw powder is in the range of 490–620°C, which is higher than the range of 350–430°C observed in the milled powder. The XRD results for the hydrogen-reduced powders indicated that only the diffraction lines for Mo are observed in the raw powder, whereas the main peak in the milled powder corresponded to Mo, and the peaks of Mo<sub>2</sub>C and Fe<sub>3</sub>Mo<sub>3</sub>C were visible as minor phases. The activation energies for the raw powder were determined to 104.4 kJ/mol and 97.5 kJ/mol depending on reduction steps of MoO<sub>3</sub>. In the ball-milled powders, the activation energies for the reduction peaks were measured to be 148.8–167.1 kJ/mol. The difference in activation energies was explained by the reaction of Fe and C impurities in the ball-milled powder with Mo to form carbides.

#### Acknowledgement

This research was supported by Seoul National University of Science and Technology.

#### REFERENCES

- [1] P. Garg, S.-J. Park, R.M. German, Effect of die compaction pressure on densification behavior of molybdenum powders. *Int. J. Refract. Met. Hard Mater.* **25**, 16–24 (2007). DOI: <https://doi.org/10.1016/j.ijrmhm.2005.10.014>
- [2] J.H. Lee, K.-J. Lee, Characterization of Compacted and pressureless sintered parts for molybdenum oxide powder according to hydrogen reduction temperature. *J. Powder Mater.* **31**, 336–341 (2024). DOI: <https://doi.org/10.4150/jpm.2024.00241>
- [3] D.C. Blaine, J.D. Gurosik, S.J. Park, D.F. Heaney, R.M. German, Master sintering curve concepts as applied to the sintering. *Metall. Mater. Trans. A.* **37**, 715–720 (2006).
- [4] B. Mouawad, M. Soueidan, D. Fabrègue, C. Buttay, V. Bley, B. Al-lard, H. Morel, Full densification of molybdenum powders using spark plasma sintering. *Metall. Mater. Trans. A.* **43**, 3402–3409 (2012). DOI: <https://doi.org/10.1007/s11661-012-1144-2>
- [5] H. Hofmann, M. Grosskopf, M. Hofmann-Antenbrink, G. Petzow, Sintering behaviour and mechanical properties of activated sintered molybdenum. *Powder Metall.* **29**, 201–206 (1986). DOI: <https://doi.org/10.1179/pom.1986.29.3.201>
- [6] S.H. Kim, D.-G. Kim, M.S. Park, Y.I. Seo, Y.D. Kim, Sintering kinetics analysis of molybdenum nanopowder in a non-isothermal process. *Met. Mater. Int.* **17**, 63–66 (2011). DOI: <https://doi.org/10.1007/s12540-011-0209-x>
- [7] R. Ohser-Wiedemann, U. Martin, H.J. Seifert, A. Müller, Densification behaviour of pure molybdenum powder by spark plasma sintering. *Int. J. Refract. Met. Hard Mater.* **28**, 550–557 (2010). DOI: <https://doi.org/10.1016/j.ijrmhm.2010.03.003>
- [8] Y. Kim, J.Y. Kim, J.W. Choi, E.S. Lee, S.-T. Oh, Morphology modification of MoO<sub>3</sub> powders by hydrogen reduction and re-oxidation process. *Arch. Metall. Mater.* **70**, 1119–1122 (2025). DOI: <https://doi.org/10.24425/amm.2025.154453>
- [9] J.-G. Ku, J.-M. Oh, H. Kwon, J.-W. Lim, High-temperature hydrogen-reduction process for the preparation of low-oxygen Mo powder from MoO<sub>3</sub>. *Int. J. Hydrog. Energy.* **42**, 2139–2143 (2017). DOI: <https://doi.org/10.1016/j.ijhydene.2016.09.004>
- [10] H.E. Kissinger, Reaction kinetics in differential thermal analysis, *Anal. Chem.* **29**, 1702–1706 (1957).
- [11] L. Wang, G.-H. Zhang, K.-C. Chou, Mechanism and kinetic study of hydrogen reduction of ultra-fine spherical MoO<sub>3</sub> to MoO<sub>2</sub>, *Int. J. Refract. Met. Hard Mater.* **54**, 342–350 (2016). DOI: <https://doi.org/10.1016/j.ijrmhm.2015.09.003>
- [12] J. Dang, G.-H. Zhang, K.-C. Chou, Study on kinetics of hydrogen reduction of MoO<sub>2</sub>, *Int. J. Refract. Met. Hard Mater.* **41**, 356–362 (2013). DOI: <https://doi.org/10.1016/j.ijrmhm.2013.05.009>
- [13] M. Saghafi, A. Ataie, S. Heshmati-Manesh, Effects of mechanical activation of MoO<sub>3</sub>/C powder mixture in the processing of nano-crystalline molybdenum. *Int. J. Refract. Met. Hard Mater.* **29**, 419–423 (2011). DOI: <https://doi.org/10.1016/j.ijrmhm.2010.12.012>
- [14] A.M. Baghdasaryan, O.M. Niazryan, H.L. Khachatryan, S.L. Kharatyan, DTA/TGA study of molybdenum oxide reduction by Mg/Zn & Mg/C combined reducers at non-isothermal conditions. *Int. J. Refract. Met. Hard Mater.* **51**, 315–323 (2015). DOI: <https://doi.org/10.1016/j.ijrmhm.2015.04.037>